Applied Mathematics and Computation 235 (2014) 8–16

Contents lists available at ScienceDirect

Applied Mathematics and Computation

journal homepage: www.elsevier.com/locate/amc

Some numerical estimations of energy levels on a model for a graphene ribbon in a magnetic field

A. Dobry [a], O. Fojón [a], M. Gadella [b,*], L.P. Lara [a]

[a] Department of Physics, Facultad de Ciencias Exactas, Ingeniería y Agrimensura, Universidad Nacional de Rosario, Argentina
[b] Department of FTAO, Facultad de Ciencias, University of Valladolid, Paseo Belén 7, 47011 Valladolid, Spain

ARTICLE INFO

Keywords:
Graphene ribbons
Dirac equation
Averaging method

ABSTRACT

We use the averaging method in order to obtain the values of the energy levels of a graphene ribbon under a magnetic field with some given conditions. We contrast the efficiency of the method with other methods for two different choices of the magnetic field.

1. Introduction

The need of numerical methods to obtain the energy spectrum of a given Hamiltonian H is out of question since in most of cases it cannot be obtained explicitly by pure analytical methods. Usually the evaluation of the eigenvalues of H can be done through the numerical resolution of a problem of Sturm–Liouville type. In the present article, we use a version of the averaging method [1] for non-periodic systems [2] in order to perform a numerical determination of the eigenvalues of a system with discrete spectrum. We show evidence that this method is rather effective, at least for low energy levels.

In fact, we use this method for the numerical determination of the spectrum in a system which is not governed by the Schrödinger equation by instead by a slightly different one, the Dirac–Weyl equation applied to the graphene, where as in a typical Sturm–Liouville problem, boundary conditions will also be given [3].

The graphene is a two dimensional layer of graphite, which has received an enormous attention as is expected to be an appropriate material to develop electronic devices [4–6]. From a physical point of view, the interest is focused in the study of the behavior of electrons in graphene strips or ribbons. This study is performed by assuming that the behavior of each singular electron is governed by a massless Dirac equation.

Motivated by the analysis of physical properties of the electrons confined in graphene ribbons, a model of graphene electrons on perpendicular magnetic field has been considered by several authors [7–9]. In these models for the graphene, an electron confined in a graphene ribbon moves with an effective Fermi speed of $v_F = c/300$, where c is the speed of light in the vacuum. Its effective Hamiltonian has the form [5]:

$$H = v_F \boldsymbol{\sigma} \cdot \left(\mathbf{p} + \frac{\mathbf{e}}{\mathbf{c}}\mathbf{A}\right), \tag{1}$$

where $\boldsymbol{\sigma} = (\sigma_x, \sigma_y)$, σ_x and σ_y being the Pauli matrices, e the electron charge, $\mathbf{A} = (A_x(x,y),\ A_y(x,y), 0)$ the potential vector due to an external magnetic field and $\mathbf{p} = -i\hbar(\partial_x, \partial_y)$, the two dimensional momentum operator. Note that, since the magnetic field is $\mathbf{B} = \nabla \times \mathbf{A}$, then it has only a nonvanishing z-component, which we are assuming to be perpendicular to the ribbon. Under the mentioned conditions, the behavior of one electron is governed by an equation of Dirac–Weyl type, which is:

* Corresponding author.
E-mail addresses: manuelgadella1@gmail.com, gadella@fta.uva.es (M. Gadella).

http://dx.doi.org/10.1016/j.amc.2014.02.060
0096-3003/

$$v_F \boldsymbol{\sigma} \cdot \left(\mathbf{p} + \frac{\mathbf{e}}{\mathbf{c}}\mathbf{A}\right)\Phi(x,y,t) = i\hbar\frac{\partial\Phi(x,y,t)}{\partial t}, \tag{2}$$

where t is time and (x,y) coordinates on the ribbon. We are interested on the stationary states. Since Eq. (2) is linear, we can use separation of variables so as to obtain solutions of the form $\Phi(x,y,t) = \Psi(x,y)e^{iEt/\hbar}$, where $\Psi(x,y)$ is solution of the following time independent Dirac–Weyl equation:

$$v_F\left[\boldsymbol{\sigma} \cdot \left(\mathbf{p} + \frac{\mathbf{e}}{\mathbf{c}}\mathbf{A}\right)\right]\Psi(x,y) = E\Psi(x,y). \tag{3}$$

This is a two components equation, i.e., $\Psi(x,y)$ is a vector whose components depend on the coordinates (x,y), i.e., $\Psi(x,y) = (\phi_1(x,y),\ \phi_2(x,y))$. The configuration space is a stripe in our case so that $0 \leqslant x \leqslant L$ and $-\infty < y < \infty$. Then, Eq. (3) splits into two coupled first order differential equations of the form:

$$-i\left(\partial_x + i\frac{eA_x}{c\hbar} - i\partial_y + \frac{eA_y}{c\hbar}\right)\phi_2(x,y) = \mathcal{E}\phi_1(x,y), \tag{4}$$

$$-i\left(\partial_x + i\frac{eA_x}{c\hbar} + i\partial_y - \frac{eA_y}{c\hbar}\right)\phi_1(x,y) = \mathcal{E}\phi_2(x,y), \tag{5}$$

with $\mathcal{E} = E/(v_F\hbar)$.

System (4, 5) is already rather complicated and, in order to obtain solutions, a simplification is in order. Following [10], we shall henceforth assume that the components of the potential vector $\mathbf{A}$ depend only on the variable x and that the x component of $\mathbf{A}$ vanishes, so that $\mathbf{A} = (0, A_y(x), 0)$ and $\mathbf{B} = (0, 0, B(x))$ with $B(x) = dA_y(x)/dx$. This is justified by choosing an magnetic field with a translational symmetry along the y direction [10]. Then, due to the linearity of (3), $\Psi(x,y)$ can be factorized in functions on the variables x and y, so that its solution has the form $\Psi(x,y) = e^{iky}(\psi_1(x),\ \psi_2(x))$, where k is a constant. With this choice, Eqs. (4) and (5) become, respectively:

$$\left(\frac{d}{dx} + k + \frac{e}{c\hbar}A_y(x)\right)\psi_2(x) = \mathcal{E}\psi_1(x), \tag{6}$$

$$\left(-\frac{d}{dx} + k + \frac{e}{c\hbar}A_y(x)\right)\psi_1(x) = \mathcal{E}\psi_2(x). \tag{7}$$

Now, the goal is to discuss a method to obtain numerically the values of $\mathcal{E}$ for given boundary conditions.

This paper is organized as follows: In Section 2, we pose the problem in precise terms with showing the differential equations object of our study. In Section 3, we introduce our method of calculation of the eigenvalues of the energy, in which the characteristics of this model for the graphene has been taken into account. In Section 4, we apply it to particular boundary conditions and analyze the results. Next, we make a comment on an alternative to Eqs. (10) and (11), showed in Section 2, so as to obtain the energy levels.

2. Second order equations

Let us go back to Eqs. (6) and (7). First of all, let us note that these equations are invariant with respect to the following scale changes (here $\mapsto$ means "changes to"): $x \mapsto x/L$, $\mathcal{E} \mapsto L\mathcal{E}$, $A_y \mapsto LA_y$, $k \mapsto Lk$. With this scale changes, one has that $0 \leqslant x \leqslant 1$ and boundary conditions to fix solutions of (6, 7) should be given by fixing values of solutions at either 0 or 1 or both. In addition, the equations are also invariant with respect to the following changes: $A_y \mapsto -A_y$, $k \mapsto -k$, $\mathcal{E} \mapsto -\mathcal{E}$, $\psi_{1,2} \mapsto \psi_{2,1}$.

Note that Eqs. (6,7) are also invariant under the transformation $A_y \mapsto A_y + \alpha$ together with $k \mapsto k + \frac{c\hbar}{e}\alpha$, so that the spectrum of values of $\mathcal{E}$ does not depend of the gauge used.

First of all, let us consider the trivial case in which $\mathcal{E} = 0$. Then, the respective solutions are given by

$$\psi_2(x) = A_2 \exp\left\{-\int\left[k + \frac{e}{c\hbar}A_y(x)\right]dx\right\} \tag{8}$$

$$\psi_1(x) = A_1 \exp\left\{\int\left[k + \frac{e}{c\hbar}A_y(x)\right]dx\right\}, \tag{9}$$

where $A_i,\ i = 1,2$ are arbitrary constants that can be fixed by assigning boundary values to $x = 0$ and $x = 1$.

Needless to say that the interesting case is $\mathcal{E} \neq 0$. Then, Eqs. (6) and (7) can be obviously transformed into the following pair of second order differential equations:

$$\left(-\frac{d^2}{dx^2} + \left(k + \frac{e}{c\hbar}A_y(x)\right)^2 + \frac{e}{c\hbar}A_y'(x)\right)\psi_1(x) = \mathcal{E}^2\psi_1(x), \tag{10}$$

$$\left(-\frac{d^2}{dx^2} + \left(k + \frac{e}{c\hbar}A_y(x)\right)^2 - \frac{e}{c\hbar}A_y'(x)\right)\psi_2(x) = \mathcal{E}^2\psi_2(x). \tag{11}$$

Recall that $0 \leqslant x \leqslant 1$. To determine solutions we need to impose some boundary conditions. They are obtained by taking into account the following conditions:

(i) The flux current should vanish in the direction perpendicular to the edges.
(ii) The flux current in the direction of the edges should be continuous. Then, no current flow should exist over the edges.

First of all, let us assume that we can choose $\psi_1(x)$ and $\psi_2(x)$ real. This is possible if the chosen boundary conditions define a self adjoint determination of the Hamiltonian, as given by the operator in front of $\psi_{1,2}(x)$ in (10) and (11). Boundary conditions chosen below determine this self adjointness (a discussion on the self adjoint extensions of the Hamiltonian is beyond the scope of the present paper, see [11,12]). This goes if we choose one of the following boundary conditions: $\psi_1(0) = \psi_1(1) = 0$, $\psi_2(0) = \psi_2(1) = 0$, $\psi_1(0) = \psi_2(1) = 0$ or $\psi_2(0) = \psi_1(1) = 0$. Then, as $j_x \propto i(\psi_1^*\psi_2 - \psi_2^*\psi_1)$, condition (i) is automatically fulfilled for $0 < x < 1$. Regarding condition (ii), we have $j_y \propto (\psi_1^*\psi_2 + \psi_2^*\psi_1) = 2\psi_1\psi_2$ for real ψ_1 and ψ_2.

In order to solve the eigenvalue problem we have posed, we can proceed into two alternative ways: Either: 1.- We use some boundary conditions for $\psi_1(x)$, for instance $\psi_1(0) = \psi_1(1) = 0$ to solve (10) to obtain $\mathcal{E}$ and $\psi_1(x)$ fulfilling these boundary conditions. Then, (7) gives us $\psi_2(x)$. Or: 2.- We provide boundary conditions for $\psi_2(x)$ at 0 and 1, determine $\mathcal{E}$ and $\psi_2(x)$ from (11) and, finally, we obtain $\psi_1(x)$ from (6). Both procedures are equivalent as they give the same results.

Observe that, although Eqs. (10, 11) look like independent, they are not as one can conclude from our above comments on the resolution procedures. Once we have solved the eigenvalue problem for either (10) or (11), the other function comes from (7) or (6) respectively. A simple analysis shows that Eqs. (10) and (11) together give the same solutions as (6, 7).

If the vector potential is linear, the determination of the two components wave function $(\psi_1(x), \psi_2(x))$ solutions is analytic, but this is not true for the case of the energy levels with the exception of the particular case of a constant potential.

Henceforth, we fix units so that $e = \hbar c$.

Both Eqs. (10) and (11) can be written in the following compact form:

$$z''(x) + \left(\mathcal{E}^2 - \left(k + A_y(x)\right)^2 \mp A_y'(x)\right)z(x) = 0, \tag{12}$$

where $z(x)$ is either $\psi_1(x)$ (with sign $-$ before $A_y'(x)$) or $\psi_2(x)$ (with sign $+$ before $A_y'(x)$). As stated before, the objective of the present paper is to obtain numerical approximations of the spectrum of energies of the model described above under different boundary conditions. We undergo this task in the next sections.

3. Solving the second order equations

Let us consider Eq. (10) in the form (12) with $z(x) = \psi_1(x)$ and use the boundary conditions $z(0) = z(1) = 0$. Our goal is to obtain reasonable approximations for both the eigenvalue $\mathcal{E}$ and the eigenfunction $z(x)$.

In order to obtain approximate solutions, we use a modification of the well known averaging method [1], valid for non-periodic solutions, that can be explained as follows: Let us consider the following differential equation:

$$y''(x) + (a - f(x))y(x) = 0, \tag{13}$$

where a is a constant and $f(x)$ is a function differentiable up to some order, defined on a given compact interval $\alpha \leqslant x \leqslant \beta$. On this interval, let us approximate (13) by

$$z''(x) + (a - \langle f(x)\rangle)z(x) = 0, \tag{14}$$

where

$$\langle f(x)\rangle = \frac{1}{\beta - \alpha}\int_\alpha^\beta f(x)\,dx \tag{15}$$

is the average of $b(x)$ on the given interval. Let x^* be a point in the interval such that $f(x^*) = \langle f(x)\rangle$ and use the Taylor theorem on the solutions of Eqs. (13) and (14) around x^*. The results are, respectively

$$y(x) = y(x^*) + y'(x^*)(x - x^*) - \frac{1}{2}(a - f(x^*))y(x^*)(x - x^*)^2 - \frac{1}{6}(a - f(x^*))y(x^*)(x - x^*)^3 - \frac{1}{6}f'(x^*)(x - x^*)^3 + \cdots \tag{16}$$

and

$$z(x) = z(x^*) + z'(x^*)(x - x^*) - \frac{1}{2}(a - f(x^*))z(x^*)(x - x^*)^2 - \frac{1}{6}(a - f(x^*))z(x^*)(x - x^*)^3 + \cdots \tag{17}$$

We observe that the solutions of (13) and (14) are identical up to order two. Beyond this order, the smaller the derivatives of $f(x)$ at x^*, the better is the approximation resulting of the replacement of (13) by (14).

Let us use this idea to solve our problem. Now, Eq. (12), with $-A_y'(x)$, will play the role of Eq. (13). Then, Eq. (14), with the corresponding boundary conditions at the borders $x = 0$ and $x = 1$ is

$$z''(x) + \omega^2 z(x) = 0, \quad z(0) = z(1) = 0, \tag{18}$$

with

$$\omega^2 := \left\langle \mathcal{E}^2 - \left(k + A_y(x)\right)^2 - A_y'(x) \right\rangle. \tag{19}$$

Here, $f(x) = \mathcal{E}^2 - \left(k + A_y(x)\right)^2 - A_y'(x)$ and $\langle f(x)\rangle = \int_0^1 f(x)\,dx$. The solutions of (18) with the given boundary conditions are well known and gives $\omega = n\pi$, with $n = 0, 1, 2\ldots$. This shows that

$$n^2\pi^2 = \mathcal{E}^2 - \left\langle \left(k + A_y(x)\right)^2 \right\rangle - \left\langle A_y'(x) \right\rangle, \tag{20}$$

which gives an approximation for the energy values, that henceforth will be labeled as $\mathcal{E}_n$, of (12) (with sign minus):

$$\mathcal{E}_n \simeq \pm\sqrt{\left\langle \left(k + A_y(x)\right)^2 \right\rangle + \left\langle A_y' \right\rangle + \pi^2 n^2}. \tag{21}$$

Thus, we observe that the dynamics of a particle with zero mass and governed by the Dirac–Weyl equation possesses a spectrum, whose set of squared eigenvalues resembles the spectrum of a particle with mass on a infinite square well governed by the Schrödinger equation.

3.1. Averaging

Eq. (21) already represents an interesting approximation to the energy levels. Now, we use an improvement of this result based in the averaging method [1]. Consider the general solution of Eq. (18) and replace the arbitrary constants by unknown functions on the variable x:

$$z(x) = y_1(x)\cos(\omega x) + y_2(x)\sin(\omega x), \tag{22}$$

and write the derivative of $z(x)$ as

$$z'(x) = -\omega y_1(x)\sin(\omega x) + \omega y_2(x)\cos(\omega x). \tag{23}$$

These functions $y_i(x),\ i = 1, 2$ have been introduced in order to modulate the harmonic response. Let us assume that the new frequency has the form $\omega_n = n\pi + \alpha_n$, where the constant α_n should depend on n. Then, the expression for the energy levels become

$$\mathcal{E}^2 = (n\pi + \alpha_n)^2 + \left\langle \left(k + A_y(x)\right)^2 + A_y' \right\rangle. \tag{24}$$

The value of α_n will be determined by the condition $z(1) = 0$. With this choice, Eq. (12), where we are always taken the minus sign, takes the following form:

$$z''(x) + \left\{ (n\pi + \alpha_n)^2 + \left\langle \left(k + A_y\right)^2 + A_y'(x) \right\rangle - \left(k + A_y(x)\right)^2 - A_y'(x) \right\} z(x) = 0. \tag{25}$$

Now, take the formal derivative of (22) with respect to x and compare it with (23). This gives the following result:

$$y_1'(x)\cos(\omega x) + y_2'(x)\sin(\omega x) = 0. \tag{26}$$

Then, replace ω by $\omega_n = n\pi + \alpha_n$ in (22), (23) and (26). Derive (23) with respect to x and replace the result in (25) so as to obtain the following expression:

$$-\omega_n y_1'(x)\sin(\omega x) + \omega_n y_2'(x)\cos(\omega x) + \left\{ \left\langle \left(k + A_y\right)^2 + A_y'(x) \right\rangle - \left(k + A_y(x)\right)^2 - A_y'(x) \right\} z(x) = 0, \tag{27}$$

where $z(x)$ is given by (22) with ω replaced by $\omega_n = n\pi + \alpha_n$. This equation along to (26) (with ω_n) provides us with a system of linear equations with indeterminates $y_i'(x),\ i = 1, 2$. Its solution is given by

$$y_1'(x) = -\frac{\omega_n^2 - \mathcal{E}^2 + \left(k + A_y(x)\right)^2 + A_y'(x)}{\omega_n} \times \left(\cos(\omega_n x)\sin(\omega_n x) y_1(x) + \sin^2(\omega_n x) y_2(x) \right), \tag{28}$$

$$y_2'(x) = -\frac{\omega_n^2 - \mathcal{E}^2 + \left(k + A_y(x)\right)^2 + A_y'(x)}{\omega_n} \times \left(\cos^2(\omega_n x) y_1(x) + cos(\omega_n x)\sin(\omega_n x) y_2(x) \right). \tag{29}$$

The next step is a simplification: we average the coefficients of $y_i(x),\ i = 1, 2$, in the right hand sides of (28) and (29) on the interval $[0, 1]$. Note that the resulting coefficients do not vanish due to the presence of products of sines and cosines. Then, if we denote the matrix vector $Y(x)$ as $Y^T(x) = (y_1(x),\ y_2(x))$, where here Y^T means transpose of Y, we can write

$$Y'(x) = MY(x). \tag{30}$$

Our objective is to determine an approximate particular solution of (22) with boundary conditions $z(0) = z(1) = 0$. To accomplish this, we need to find particular solutions of (28, 29) with suitable initial conditions and then use these solutions in (22). Then, the condition $z(1) = 0$ will give the values of α_n. The initial conditions for $y_i(x),\ i = 1, 2$ are $y_1(0) = z(0) = 0$ and $y_2(0) = z'(0)/\omega_n$. The value of $z'(0)$ is not known, but its value is not relevant for our discussion. In fact, the particular solution of (30) with the given initial conditions has the following form:

$$Y(x) = \exp\{Mx\}\begin{pmatrix} 0 \\ z'(0)/\omega_n \end{pmatrix}, \quad \exp\{Mx\} = \begin{pmatrix} y_{11}(x) & y_{12}(x) \\ y_{21}(x) & y_{22}(x) \end{pmatrix}, \tag{31}$$

where the matrix elements y_{ij} depend on both x and ω. This gives

$$y_1(x) = y_{12}(x)z'(0)/\omega_n; \quad y_2(x) = y_{22}(x)z'(0)/\omega_n. \tag{32}$$

If we use this result in (22), we obtain

$$z(x) = [y_{12}(x)\cos(\omega_n x) + y_{22}(x)\sin(\omega_n x)]z'(0)/\omega. \tag{33}$$

Note that $z'(0) \neq 0$, otherwise $z(x)$ would be identically zero. Then, the condition $z(1) = 0$ gives

$$y_{12}(1)\cos(\omega_n) + y_{22}(1)\sin(\omega_n) = 0. \tag{34}$$

This is the equation we need to determine α_n, which does not depend of the value of $z'(0)$.

As a minor remark, we note that if $\left\langle (k + A_y)^2 + A'_y(x) \right\rangle - (k + A_y(x))^2 - A'_y(x) = 0$, then $y'_{1,2}(x) \equiv 0$ and therefore in (18) we have $\omega_n = n\pi$. This is one reason to conjecture that a good approximation would be achieved whenever $(k + A_y(x))^2 - A'_y(x) \approx \left\langle (k + A_y)^2 + A'_y(x) \right\rangle$ on the interval $[0, 1]$.

4. Some particular cases

Next, we analyze two particular cases: constant magnetic field and periodic potential.

4.1. Constant magnetic field

Now, let us assume that the magnetic field is constant. Then, the vector potential is $A_y(x) = B_0 x + \beta$, where B_0 and β are constants. In this case, the equation given in (12), with sign minus, when one uses the boundary condition $z(0) = 0$, it admits an explicit solution in terms of Parabolic-Cylinder functions which is

$$z(x) = D_{\frac{\varepsilon^2}{2B_0}-1}\left(\sqrt{\frac{2}{B_0}}(k + \beta + B_0 x)\right) \times D_{\frac{\varepsilon^2}{2B_0}-1}\left(\sqrt{-\frac{2}{B_0}}(k + \beta)\right) \times \left\{D_{\frac{\varepsilon^2}{2B_0}-1}\left(\sqrt{\frac{2}{B_0}}(k + \beta)\right)\right\}^{-1}$$
$$+ D_{-\frac{\varepsilon^2}{2B_0}}\left(\sqrt{-\frac{2}{B_0}}(k + \beta + B_0 x)\right) \tag{35}$$

In order to obtain the eigenvalue, we solve numerically the equation $z(1) = 0$. These numerical values are quite well approximated by those obtained by using the method proposed in Section 3.1, as we determined by numerical tests. These numerical experiments, shown that the lowest eigenvalues obtained by means of (21) are quite close to the exact ones. The explicit expression of (21) in our case is

$$\mathcal{E}_{k,n} \approx \pm\sqrt{(k + \beta)^2 + B_0(1 + k + \beta + B_0/3) + \pi^2 n^2}. \tag{36}$$

In Fig. 1, the dots denote the energy levels. In the abscissa, we have the values of n and in the ordinate we have the corresponding values of the energy for the choices $k = 2$, $B_0 = 1$ and $\beta = 5$. The curve in red that joins the dots is given by (21) with $A_y(x) = B_0 x + \beta$. Note that for our level of precision, the curve crosses the points. Although we have not been able to give a realistic bound of error, this gives an idea of the accuracy of our method.

Eq. (36) shows that the approximate expression for the energy levels depends on the gauge constant β. This is, in principle, quite surprising. Experimentally, one measures the differences between levels. Now, this difference may depend on the chosen value for β. Take two different values β_1 and β_2 and call $\mathcal{E}^{(1)}_{k,n}$ and $\mathcal{E}^{(2)}_{k,n}$ the values of (36) obtained with these two values of β respectively.

Then, let us calculate the difference between the squares of the values of the energy, as determined by (36), in the transitions from (k_1, n) to (k_2, m) using first β_1 and then β_2. Since

$$\mathcal{E}^2_{k_2,n} - \mathcal{E}^2_{k_1,n} = 2A_y(k_2 - k_1) + k_1^2 + k_2^2, \tag{37}$$

one has

$$\left(\left[\mathcal{E}^{(2)}_{k_2,m}\right]^2 - \left[\mathcal{E}^{(2)}_{k_1,n}\right]^2\right) - \left(\left[\mathcal{E}^{(1)}_{k_2,m}\right]^2 - \left[\mathcal{E}^{(1)}_{k_1,n}\right]^2\right) = -2(k_1 - k_2)(\beta_1 - \beta_2). \tag{38}$$

Note that this result does not depend on n, although it depends on the gauge constant β. This result emerges not only by making use of (36) to obtain the energy values, but also from direct numerical integration from $z(1) = 0$. This result is somehow surprising as it may mean that the gauge and therefore the vector potential may have physical relevance.

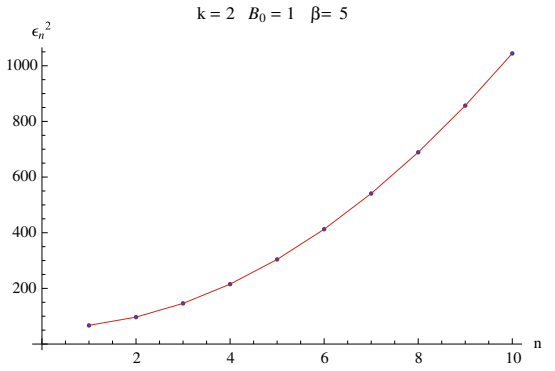

Fig. 1. The dots are the energy levels for $k = 2$, $B_0 = 1$ and $\beta = 5$. The curve is the graphics for (21).

4.2. Periodic potential

In this second example, the complete above procedure is not necessary and can be drastically simplified, as we shall see. Assume that the magnetic field is periodic and has translational symmetry with respect to the direction of y. Then, it admits a vector potential of the form $A_y(x) = A_0 \sin(\omega_m x)$, with $\omega_m = m\pi,\ m = 1, 2, \ldots$. In this case, Eq. (21) gives

$$\mathcal{E}_{k,n} \simeq \pm\sqrt{\frac{1}{2}A_0 + k^2 + \pi^2 n^2}, \tag{39}$$

for m even and

$$\mathcal{E}_{k,n} \simeq \pm\sqrt{\frac{1}{2}A_0^2 + k^2 + 4A_0\frac{k}{m\pi} + \pi^2 n^2} \tag{40}$$

for m odd. Here, we impose a unique initial condition $z(0) = 0$, which gives the following solution for the equation in (18):

$$z(x) = C\sin(n\pi x), \tag{41}$$

where C is an arbitrary constant.

In principle, this is an approximation for which we do not have an explicit expression for the error estimation. We recall that a good result can be expected provided that $\left\langle (k + A_y)^2 + A_y'(x)\right\rangle - (k + A_y(x))^2 - A_y'(x)$, is small. Numerical experiments permit us to compare the results obtained with this approximation with those which have been obtained in the method proposed in [16]. We find that for $A_0 < 10$ and $1 \leqslant m \leqslant 10$, there is a very reasonable coincidence between both results with values of n bigger than 2 ($n > 2$), with an error bound of the order of 5%. The corresponding eigenfunctions approximate quite well to the $z(x)$.

Now and within the range of the parameters as in the previous paragraph, let us use the method as described previously in the present section. The values obtained were similar to those obtained using the ideas just given above. Therefore, in this case, the approximation given by Eq. (18) is clearly sufficient.

On Fig. 2, we represent the spectrum obtained with the use of the following parameters: $A_0 = 5,\ k = 2$ and $m = 2$. Red spots are those given by (21) and blue spots are determined numerically using the Taylor method. The horizontal axis represents the variable n and the vertical axis $\mathcal{E}^2$, the square of the energy values.

In order to compare solutions given by Eqs. (41) and (22), we give here just an example. For the seventh energy label, with energy given by $\mathcal{E} = 500.518$, we obtain using (24):

$$z(x) = 0.0454728\sin(21.9911x), \tag{42}$$

while the result obtained with (22) is

$$\begin{aligned} z(x) = {} & 0.0448296\sinh(0.00017877x)\cos(22.0004x) + (0.0529599)\cosh(0.000178778x) \\ & - 0.0075061\exp(0.000178778)\sin(22.0004x). \end{aligned} \tag{43}$$

Comparing (41) and (42), we conclude that numerical differences between these two expressions are very small. In order to determine the error, we use the expression $D = \left\langle (z_{\text{numerical}} - z_a)^2\right\rangle$. We obtain for D, 0.0000162716 for (41) and 0.0000167253 for (42). As we can see the differences are of order 10^{-7}.

A simple remark: let us consider either the boundary conditions (often called the zig-zag conditions) $z_1(0) = z_2(1) = 0$ or $z_2(0) = z_1(1) = 0$ and obtain the spectrum numerically using the method in [16]. Then, for each pair of two consecutive

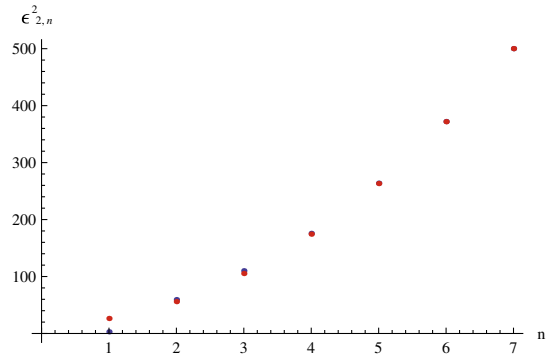

Fig. 2. Spectrum obtained with $A_0 = 5$, $k = 2$ and $m = 2$.

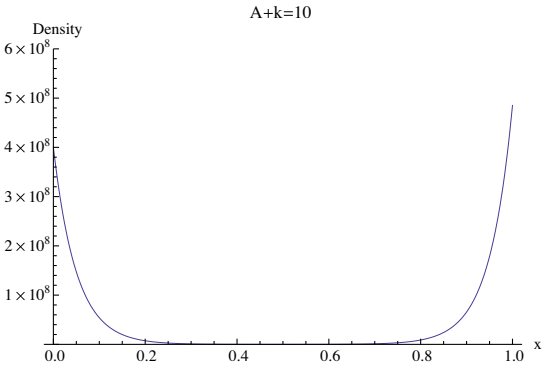

Fig. 3. Probability density for $A_y + k = 10$.

values of the energy with respect to the homogeneous conditions ($z_i(0) = z_i(1) = 0,\ i = 1, 2$), there is one value of the energy with respect to these zig-zag conditions.

5. Concluding remarks

In this paper we have developed a numerical method to solve a Dirac–Weyl equation in the presence of a magnetic field in a two dimensional band. We checked the method against exact solution or other numerical method when the exact solution does not exist.

Our results should be taken as a starting points for the study of other realistic situation in graphene nanoribbons. Related to this question, the boundary condition chosen in Section 4 belongs to the family proposed in [3]. As have previously discussed, they give vanishing flux of current perpendicular to the edges of the band. They also produce no current flow over the edges.

Other boundary condition could be necessary in order to account different realizations of graphene nanoribbons. For example the so called zig-zag edges correspond to $\psi_1(0) = \psi_2(1) = 0$ or $\psi_2(0) = \psi_1(1) = 0$ in our notation. This problem is also solvable by the method proposed in the present paper.

Different spatial configuration for the magnetic field are also possible and worthy to be applied to the graphene. The most promising possibility consists in simulating a magnetic field by applying strains to the sample [13]. In this way, a periodic magnetic field as we studied in Section 4.2 could be in principle produced by supporting graphene on a corrugated substrate [14,15].

Studying different boundary conditions and different spatial dependence of the magnetic field will be the subject of a future work.

Acknowledgments

Partial financial support is acknowledged to the Spanish Ministry of Education (Projects MTM2009-10751 and PR2011-0343), also to the Project UNR-ING 195, PIP 11220090100392 of CONICET, and PICT R 1776 of the ANPCyT (Argentina).

Appendix A. A remark

Here, we propose another method to obtain the values $\mathcal{E}$ of the energy spectrum. Let us start with equations (6, 7) and use the following change to define a new unknown function $f(x)$:

$$f(x) := \psi_1(x) \exp\left\{-\int \big(k + A_y(x)\big)\, dx\right\}. \tag{A.1}$$

Then, take the resulting expression for $\psi_1(x)$ into Eq. (7) in order to obtain a similar formula for $\psi_2(x)$:

$$\psi_2(x) = -\frac{1}{\mathcal{E}} f'(x) \exp\left\{\int \big(k + A_y(x)\big)\, dx\right\}. \tag{A.2}$$

Use (43) and (A.1) into (7). This gives:

$$f''(x) + 2\big(k + A_y(x)\big)f'(x) + \mathcal{E}^2 f(x) = 0. \tag{A.3}$$

This equation is simpler than (10) and (12). In order to obtain the energy spectrum, we have to impose boundary conditions. The simplest boundary conditions are $\psi_1(0) = \psi_1(1) = 0$, which gives $f(0) = f(1) = 0$. It is sufficient imposing boundary conditions on $\psi_1(x)$ in order to obtain $\psi_1(x)$ as well as $\psi_2(x)$. Note that the zeroes of $\psi_1(x)$ and $\psi_2(x)$ are the zeroes of $f(x)$ and $f'(x)$ respectively. This shows that between two consecutive zeroes of $\psi_1(x)$ there must be a zero of $\psi_2(x)$ as $f'(x)$ must be zero at some point.

One comment is in order here: Let us go back to (A.3) in which we have dropped the middle term. Then, (A.3) takes the form $f''(x) + \mathcal{E}^2 f(x) = 0$. This equation has the same spectrum (values of $\mathcal{E}$) for the boundary conditions given either by $f(0) = f(1) = 0$ or by $f'(0) = f'(1) = 0$. This approximately happens for high values of $\mathcal{E}$. Therefore, the energy levels obtained with the boundary conditions $\psi_1(0) = \psi_1(1) = 0$ and $\psi_2(0) = \psi_2(1) = 0$ respectively are quite similar in this case. Within the same approximation, if we take as boundary conditions either $f(0) = f'(1) = 0$ or $f'(0) = f(1) = 0$, the new eigenvalues are alternate with those obtained with the homogeneous conditions.

Boundary conditions of the form $f(0) = f'(1) = 0$ and $f(1) = f'(0) = 0$ give as spectrum $W_n = (2n-1)\pi/2,\ n = 1, 2, 3\ldots$. Note that two consecutive values of $\omega_n = n\pi$ contains one and only one value of W_n.

Appendix B. One comment concerning the behavior of the density

Since the current density in the direction y is given by $j_y = 2\psi_1\psi_2$, we can write an expression for it with the help of A.1,A.2:

$$j_y = -\frac{1}{\mathcal{E}} f(x)f'(x) \exp\left\{2\int (A_y(x) + k)\, dx\right\}. \tag{B.1}$$

Now, let us consider the probability density $\rho = \psi_1^2 + \psi_2^2$. Using again formulas A.1,A.2, we have:

$$\frac{d}{dx}\left(f^2(x) + \frac{1}{\mathcal{E}} f'^2(x)\right) = -\frac{4}{\mathcal{E}^2}\,(A_y(x) + k)f'^2(x). \tag{B.2}$$

Note that whenever $A_y(x) + k > 0$, the expression between parenthesis in the left hand side of (B.2) decreases and therefore if it is not balanced by the exponential term in (B.1), the density average decreases. See Fig. 3.

The property that we want to show first uses (B.1) and (B.2) to obtain the following relation:

$$j_y = -\frac{1}{\mathcal{E}} \frac{f(x)f'(x)}{f^2(x) + \frac{1}{\mathcal{E}^2} f'(x)^2}\, \rho. \tag{B.3}$$

We recall that (B.3) is well defined as $f(x)$ and $f'(x)$ cannot vanish simultaneously. Finally, using 6,7, we arrive to

$$\frac{d}{dx}\,\rho = \frac{1}{\mathcal{E}}\big(A_y(x) + k\big)\,\frac{d}{dx}\, j_y, \tag{B.4}$$

which is the desired equation. It relates the derivative of the density to the derivative of the current density.

References

[1] F. Verhulst, Nonlinear Differential Equations and Dynamical Systems, Springer, Berlin, 1990.
[2] M. Farkas, Periodic Motion, Springer, New York, 1994.
[3] C.G. Beneventano, E.M. Santangelo, Boundary conditions in the Dirac approach to graphene devices, Int. J. Mod. Phys. Conf. Ser. 14 (2012) 240–249.
[4] K.S. Novoselov, A.K. Geim, S.M. Morozov, Y. Zhang, I.V. Grigorieva, A.A. Firsov, Electric field effect in atomically thin carbon films, Science 306 (2004) 666–669.
[5] A.H. Castro Neto, F. Guinea, N.M.R. Peres, K.S. Novoselov, A.K. Geim, The electronic properties of graphene, Rev. Mod. Phys. 81 (2009) 109–162.
[6] V.N. Kotov, B. Uchoa, V.M. Pereira, F. Guinea, A.H. Neto Castro, Electron–electron interactions in graphene: current status and perspectives, Rev. Mod. Phys. 84 (2012) 1067–1125.

[7] G. Giavaras, P.A. Maksym, M. Roy, Magnetic field induced confinement–deconfinement transition in graphene quantum dots, J. Phys: Condens. Matter 21 (2009) 102201.
[8] A. Di Martino, L. Dell'Anna, R. Egger, Magnetic confinement of massless Dirac fermions in graphene, Phys. Rev. Lett 98 (2007) 066802.
[9] T.K. Ghosh, Exact solutions for a Dirac electron in an exponentially decaying magnetic field, J. Phys: Condens. Matter 21 (2009) 045505.
[10] S. Kuru, J. Negro, L.M. Nieto, Exact analytic solutions for a Dirac electron moving in graphene under magnetic field, J. Phys: Condens. Matter 21 (2009) 455305.
[11] S. Albeverio, F. Gesztesi, R. Heg-Krohn, H. Holden, Solvable Models in Quantum Mechanics, Springer, New York, 1988.
[12] S. Albeverio, P. Kurasov, Singular perturbations of differential operators, Lecture Note Series, vol. 271, London Mathematical Society, Cambridge, UK, 2000.
[13] F. Guinea, M.I. Katsnelson, A.K. Geim, Energy gaps and a zero-field quantum Hall effect in graphene by strain engineering, Nat. Phys. 6 (2010) 30–33.
[14] S. Scharfenberg, D.Z. Rocklin, C. Chialvo, R.L. Weaver, P.M. Goldbart, N. Mason, Probing the mechanical properties of graphene using a corrugated elastic substrate, Appl. Phys. Lett. 98 (2011) 091908.
[15] S. Costamagna, O. Hernandez, A. Dobry, Spectral gap induced by structural corrugation in armchair graphene nanoribbons, Phys. Rev. B 81 (2010) 115421.
[16] J.J. Alvarez, M. Gadella, L.P. Lara, The one dimensional infinite square well with variable mass. arXiv:1402.5378. <http://lanl.arxiv.org/abs/1402.5378>.